Nonlinear characterization of a bolted, industrial structure using a modal framework

Daniel R. Roettgen

Graduate Research Assistant

dan.roettgen@wisc.edu

&

Matthew S. Allen

Associate Professor

msallen@engr.wisc.edu

Department of Engineering Physics

University of Wisconsin-Madison

534 Engineering Research Building

1500 Engineering Drive

Madison, WI 53706

Abstract:

This article presents measurements from a sub assembly of an off-the-shelf automotive exhaust system containing a bolted-flange connection and uses a recently proposed modal framework to develop a nonlinear dynamic model for the structure. The nonlinear identification and characterization methods used are reviewed to highlight the strengths of the current approach and the areas where further development is needed. This marks the first use of these new testing and nonlinear identification tools, and the associated modal framework, on production hardware with a realistic joint and realistic torque levels. To screen the measurements for nonlinearities, we make use of a time frequency analysis routine designed for transient responses called the zeroed early-time fast Fourier transform (ZEFFT). This tool typically reveals the small frequency shifts and distortions that tend to occur near each mode that is affected by the nonlinearity. The damping in this structure is found to be significantly nonlinear and a Hilbert transform is used to characterize the damping versus amplitude

behavior. A model is presented that captures these effects for each mode individually (e.g. assuming negligible nonlinear coupling between modes), treating each mode as a single degree-of-freedom oscillator with a spring and viscous damping element in parallel with a four parameter Iwan model. The parameters of this model are identified for each of the structure's modes that exhibited nonlinearity and the resulting nonlinear model is shown to capture the stiffness and damping accurately over a large range of response amplitudes.
Keywords: Iwan Model, Nonlinear Detection, Nonlinear Modeling.

1. Introduction

Joints have long been known to be a significant, if not the most significant, source of damping in built up assemblies. They are also frequently the source of nonlinearity in what would otherwise be a linear structure. However, even when joints behave linearly, their linear stiffness and damping properties are difficult to predict. Hence, when updating a finite element model a significant fraction of the effort is focused on the joints. This work seeks to address the challenge of testing structures with weakly nonlinear joints by using a recently proposed framework that models the structure as a collection of uncoupled, weakly nonlinear (in the case of micro-slip) oscillators. A set of tools is presented that can be used to characterize the nonlinearity in each mode due to the joints. These tools are applied, for the first time, to measurements from an assembly from an automotive exhaust system that contains two joints with realistic geometry, gaskets, and bolt torques.

This work builds on the efforts of Segalman, and his colleagues at Sandia National Laboratories, who pursued a multi-year project in which models for mechanical joints were derived and calibrated to match experimental force-dissipation measurements [1, 2]. They showed that one can determine the parameters for each joint in a structure and employ nonlinear time integration to compute the response including the effects of the joints. This greatly increases the cost of the response predictions so model reduction strategies were explored. In applying this framework to simulate various structures, it has been noted that the resulting response is usually very nearly linear, causing one to question whether there might be an easier, less expensive way to model them. For small enough loads, mechanical joints tend to exhibit micro-slip, a phenomenon in which the joint as a whole remains intact but small slip displacements occur at the outskirts of the contact patch causing frictional energy loss in the system [1].

Towards this end, Segalman recently proposed to model each mode of a structure as independent but with an Iwan joint in parallel with the modal stiffness to capture the nonlinear damping (and to a lesser extent nonlinear

stiffness) of the joint [3]. A rigorous theoretical foundation for models with uncoupled modes such as this was developed by Eriten et al. [4], who showed that energy transfer between modes can be negligible in the presence of weak nonlinearity unless their frequencies are close. Using this framework, one can identify or model the weak nonlinearity of each mode individually. Allen and Deaner later extended Segalman's work by adding a viscous damper in parallel with the Iwan element account for the linear material damping that dominates for each mode at very small amplitudes [5] and began to more thoroughly explore the extent to which this modal approximation is accurate for real structures with several joints [6]. They used two new tools, namely the Hilbert transform algorithm developed by Sumali et al. [5, 7] and the Zeroed Early-Time FFT (ZEFFT) algorithm by Mayes & Allen [8] to characterize each mode of the structure. The ZEFFT algorithm is a simple time-frequency decomposition comparable to the short time Fourier transform or wavelet transform that allows one to quickly interrogate each mode to detect those modes that exhibit nonlinearity.

Once one has determined which modes might be behaving nonlinearly, a Hilbert transform analysis can be used to extract the instantaneous frequency and damping of each harmonic in the signal. This analysis is only applicable to single-frequency signals, and so the measurements must first be band-pass filtered to isolate a single frequency. Other researchers have instead employed empirical mode decomposition or other variants [4, 9, 10], but these algorithms are far from straightforward to use and are sometimes ineffective at separating close frequencies, so they were not pursued in this work. Once a single frequency signal has been obtained, the Hilbert transform can be computed and then the output of the Hilbert transform must be smoothed in some way so that its derivative can be found and used to estimate the time varying oscillation frequency and damping. The authors smooth the signal by fitting a polynomial to the amplitude and phase as a function of time, similar to what was done in [5, 7]; others have instead filtered the Hilbert transform [11]. Sapsis et al. recently presented another interesting alternative, in which the local maxima in the velocity and displacement were fit to a spline function and then energy measures were derived to extract the instantaneous stiffness and damping [12].

The approach used here is similar to that which was first used by Deaner et al. [5] to characterize a beam with a bolted joint. However, this work presents a new means of interpreting the dissipation in the modal Iwan model that allows one to more clearly see how the damping ratio changes with response amplitude, while still allowing power-law behavior to be identified. Specifically, while previous works [2, 5] characterized the damping in an Iwan model using the energy dissipation versus cycle versus velocity amplitude (or force), this work shows that superior information can be obtained by computing the effective damping ratio and displaying it versus log velocity

amplitude. This work also builds on the previous works by exploring whether these tools and the modal Iwan modeling framework are effective for a real industrial structure with several joints, with gaskets in the interfaces, bolts tightened to the recommended specifications, and with complicated, three-dimensional modal deformations. The effect of the input location is explored in more detail here, presenting much stronger evidence that the modal Iwan model is valid for a wide range of inputs.

It should be noted that other frameworks have been proposed for modeling structures with joints. Of particular note is the harmonic balance approach employed, for example, in [13] and the associated methods reviewed there and in related works [14]. The harmonic balance can be very computationally efficient, especially when seeking to simulate stepped-sine measurements or nonlinear frequency responses. However, some of those gains may be lost when the joint is modeled by an Iwan model with many slider elements, and harmonic balance is, of course, not as useful when impulsive loads are of interest.

2. Nonlinear Model Characterization - Theory

In order to develop a nonlinear model for a structure, one must first find a means of detecting nonlinearity in measured experimental data. In this work this is done in a two step process. First, the data is analyzed using the zeroed early-time fast Fourier transform (ZEFFT) [8] to determine which modes might exhibit nonlinearity. The ZEFFT applies the following window $w(t)$ to the time history $x(t)$, and then the FFT is computed for various truncation times t_n.

$$w(t) = \begin{cases} 0 & t \le t_n \\ 1 & t > t_n \end{cases} \tag{1}$$

This analysis is quick and simple to perform and by comparing the spectra, $\mathrm{FFT}(w(t)x(t))$, for various truncation times one can discern the type of the nonlinearity by observing how the frequency and shape of the curves change as more and more time signal is zeroed out.

After completing this initial screening process, each mode is isolated to quantify how its frequency and damping change with amplitude. A linear modal test is performed (with the structure excited at very low amplitude) and the mass normalized mode shapes are extracted from a curve fit to the measurements using standard techniques [15]. In previous works [16] a laser vibrometer was used so each response measurement was independent of all others and had to be processed separately. When the structure of interest is sufficiently massive, as is the structure used in this work, one can use accelerometers without adding significant mass or

damping (from the cables). As mentioned previously, each mode is assumed to be independent and to be manifest with approximately the same mode shape as in the linear system, so all measurements should be related to one modal response, so the following equation can be solved in a least squares sense to obtain the modal amplitude.

$$\boldsymbol{\varphi}_r \ddot{q}_r(t) = \ddot{\mathbf{x}}(t) \tag{2}$$

where $\boldsymbol{\varphi}_r$ is the rth mass-normalized mode vector, $\ddot{q}_r(t)$ is the corresponding modal response and $\ddot{\mathbf{x}}(t)$ is a vector of accelerations that were measured due to one impact with an instrumented hammer. This method allows multiple hammer strikes to be compared even from different driving point locations. Note that the mode shapes here are assumed to be real and constant which limits this method to weakly nonlinear structures.

The next step in the screening process is to quantify the change in damping with amplitude. As mentioned in the introduction, the Hilbert transform algorithm detailed in [5, 7] is used. First, an 8th order band-pass filter is used to isolate a single harmonic (mode) in the response. Then, the Hilbert transform of the mono-component signal is computed and an 8th order polynomial is fit to the time varying amplitude and phase. In essence, this approach fits the modal response, $q(t)$, to the following functional form, where $\psi_r(t)$ and $\psi_i(t)$ are 8th order polynomials in time and are, respectively, the real and imaginary parts of the time varying response model

$$\ddot{q}(t) = e^{\psi_r(t) + \mathrm{i}\psi_i(t)} \tag{3}$$

To achieve this, the analytic signal, $\ddot{Q}(t)$, is constructed as

$$\ddot{Q}(t) = \ddot{q}(t) + \mathrm{i}H\left(\ddot{q}(t)\right) \tag{4}$$

where $H()$ denotes the Hilbert transform. The real part, $\psi_r(t)$, is fit to the log of the amplitude of the analytic signal, $\psi_r(t) = \log\left|\ddot{Q}(t)\right|$, and the imaginary part is fit to its unwrapped phase, $\psi_i(t) = \arg\left(\ddot{Q}(t)\right)$.

The phase of the analytic signal gives the oscillation frequency, so the damped natural frequency was defined as its derivative in [5],

$$\omega_d(t) \triangleq \frac{d\psi_i}{dt} \tag{5}$$

which one can readily show gives the desired result for a linear time invariant system.

It is convenient to convert the response model from acceleration to velocity for the analyses that follow. The desired velocity response model can be written in a similar form, where the hats denote that this model pertains to velocity rather than acceleration.

$$\dot{q}(t) = e^{\hat{\psi}_r(t)+\mathrm{i}\hat{\psi}_i(t)} \tag{6}$$

This can be readily differentiated to obtain the following,

$$\ddot{q}(t) = \left(\frac{d\hat{\psi}_r(t)}{dt} + \mathrm{i}\frac{d\hat{\psi}_i(t)}{dt} \right) e^{\hat{\psi}_r(t)+\mathrm{i}\hat{\psi}_i(t)} \tag{7}$$

It is not trivial to relate the velocity and acceleration response models precisely, but if one recognizes that damping is small so that

$$\left(\frac{d\hat{\psi}_r(t)}{dt} + \mathrm{i}\frac{d\hat{\psi}_i(t)}{dt} \right) \approx \mathrm{i}\frac{d\hat{\psi}_i(t)}{dt} = \mathrm{i}\hat{\omega}_d(t) \tag{8}$$

then one can approximate the acceleration as follows.

$$\ddot{q}(t) \approx \mathrm{i}\hat{\omega}_d(t) e^{\hat{\psi}_r(t)+\mathrm{i}\hat{\psi}_i(t)} \tag{9}$$

This reveals that one can take $\hat{\psi}_r(t) + \mathrm{i}\hat{\psi}_i(t) \cong \psi_r(t) + \mathrm{i}\psi_i(t)$ and estimate the velocity response model by simply dividing the acceleration response model by $\omega_d(t)$, exactly as is done for a linear response. Hence, the amplitude of the velocity response will be approximated by the following.

$$\left|\dot{Q}(t)\right| \approx \frac{e^{\psi_r(t)}}{\omega_d(t)} \tag{10}$$

If the damping is high, then the approximation in the equation above will introduce some inaccuracy and a more elaborate approach must be developed. However, in the authors' experience the decay envelope estimated by the Hilbert transform always exhibits some spurious oscillation, even after smoothing with the polynomial fit, so this approach does not introduce significant uncertainty.

As was done in [5], each mode will be modeled with a single degree of freedom system with a spring, damper, and with the nonlinear joint model represented by the force exerted by the joint as shown in Fig. 1.

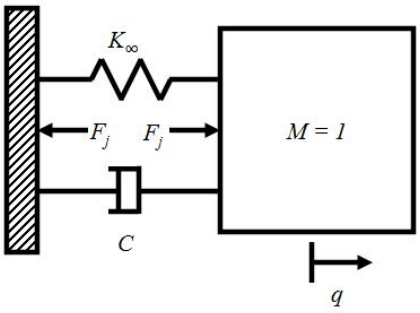

Figure 1. Schematic of SDOF model used for each modal degree of freedom

The force in the joint is given by the following,

$$F_j(t) = \int_0^\infty \rho(\phi)\left[u(t) - x(t,\phi)\right] d\phi \tag{11}$$

where F_j is the force in the joint, u is joint displacement, ρ is a kernel that characterizes the joint and x is a continuum of state variables that evolve as

$$\dot{x}(t,\phi) = \begin{cases} \dot{u} \;\text{ if }\; \left\|u - x(t,\phi)\right\| \\ \qquad \text{and }\; \dot{u}\left(u - x(t,\phi)\right) > 0 \\ 0 \quad \text{otherwise} \end{cases} \tag{12}$$

The form of the kernel, $\rho(\phi)$, is discussed in detail in [2] and can be defined by four parameters, $[F_s,\ K_T,\ \chi,\ \beta]$; where F_s is the joint force required to begin macro-slip, K_T is the stiffness in the joint, χ is related to the exponent in a power-law relationship between damping and amplitude in the micro-slip regime and β defines the shape of the dissipation curve near the transition from micro to macro-slip. When this joint model is used in a modal framework, these four parameters define the nonlinear characteristics of each mode in the system and can be obtained from experimental measurements as outlined in [5]. K_T is defined as the change in stiffness as shown in Eq. (13) where ω_n is the natural frequency when the joint is completely stuck and $\Delta\omega_n$ is the shift in natural frequency when the joint is in macro-slip.

$$\mathrm{K_T} = {\omega_n}^2 - \left(\omega_n - \Delta\omega_n\right)^2 \tag{13}$$

The measurements presented in this work are entirely from the linear or micro-slip regimes, so only those aspects of the modal Iwan model will be reviewed here. At very low amplitudes the nonlinear element acts like a linear spring and the viscous damper dominates. In the micro-slip regime the damping becomes nonlinear and

the energy dissipated per cycle, D_{Micro}, by in the single degree of system in Fig. 1 was shown in [5] to have the following form.

$$D_{\mathbf{Micro}} \approx A_{\mathbf{Iwan}} \left|\dot{Q}(t)\right|^{\chi+3} + 2\zeta_v \omega_n \left(\frac{\pi}{\omega_d}\right)\left|\dot{Q}(t)\right|^2$$
$$A_{\mathbf{Iwan}} = \frac{4R}{\left(\omega_d(t)\right)^{\chi+3}\left(\chi+3\right)\left(\chi+2\right)} \tag{14}$$

where R is a function of $\mathrm{F_s}$, $\mathrm{K_T}$ and χ and was defined in [5]. The second term is the dissipation of a linear viscous damper with damping ratio ζ_v. (This linear dissipation term is easily derived by recognizing that the power dissipated by a linear viscous damper is given by the product of the modal velocity $\dot{q}(t)$ and the modal damping force, $2\zeta_v \omega_n \dot{q}(t)$ and then the term on the right above is readily obtained by assuming that $\dot{q}(t)$ is harmonic, $\dot{q}(t) = \left|\dot{Q}(t)\right|\sin\left(\omega_d t\right)$, and integrating the power dissipated over one cycle.)

One can readily use the response model that was fit to the measurements to estimate the energy dissipated by each modal degree of freedom per cycle. First we note that, although the kinetic energy is oscillatory, its amplitude, here denoted KE, is equal to the total energy in the system and is simply

$$KE = \frac{1}{2}\left|\dot{Q}(t)\right|^2 \approx \frac{1}{2}\left(\frac{e^{\psi_r(t)}}{\omega_d(t)}\right)^2 \tag{15}$$

since the modal mass is unity. The amplitude of the kinetic energy decays slowly (i.e. with the decay envelope of the signal) so the energy dissipated per cycle is readily approximated as the slope of the kinetic energy versus time multiplied by the oscillation period. Hence,

$$D \approx \frac{2\pi}{\omega_d}\frac{dKE}{dt} \tag{16}$$

In [5], this experimentally measured dissipation was fit to the form given by Eq. (14) to estimate the parameters of the Iwan model, one of the most important being the exponent, $\left(\chi+3\right)$, of the dissipation versus amplitude. This exponent was estimated by fitting a line to the log dissipation vs. log amplitude curve estimated from the Hilbert transform. However, it was subsequently noted that the dissipation vs. amplitude curves were difficult to interrogate because, as shown in Eq. (14), the dissipation increases with the square of velocity amplitude even for a linear system, so the plot shows a slope of two even for a linear system. In this work, we remedy this by

computing the effective linear damping ratio from the measured dissipation curve. Specifically, using the term on the right in Eq. (14) as a guide, we define the measured damping ratio as

$$\zeta_{meas}(t) \triangleq \frac{D}{2\pi \left|\dot{Q}(t)\right|^2} \tag{17}$$

If the system is linear and the damping is purely viscous, then we obtain a line with $\zeta_{meas}(t) = \zeta_v / \sqrt{1-\zeta_v^2}$. The Iwan joint then produces the following damping ratio.

$$\zeta_{\mathbf{Iwan}}(t) \approx \frac{A_{\mathbf{Iwan}}}{2\pi} \left|\dot{Q}(t)\right|^{\chi+1} \tag{18}$$

Hence, one can readily estimate the power law exponent and the constant $A_{\mathbf{Iwan}}$ from the damping ratio measured using Eq. (17).

3. Experimental System - Coupled Catalytic Converters

The proposed approach was applied to a system consisting of a two aft catalytic converters for a Buick LaCrosse (Part Number: 82071258), joined to a thick metal plate as seen in Fig. 2. This same system has also been used to develop substructuring techniques, as reported in [16]. The converters were joined to the plate using the same metal gaskets (Part Number: 20893953) that are used in the actual vehicle and assembled with four bolts. The bolts in this assembly were tightened to the recommended 45 N-m torque. The frequency range of interest in these tests was 0 to 500 Hertz, which would encompass many of the low frequency modes of the exhaust system.

Figure 2. Photographs of the Catalytic Converter System

The dynamic response of the coupled system was measured using accelerometers placed at seven locations on the center plate and three locations on both converters. A modal test was completed with low level excitation using an impact hammer striking at multiple driving point locations. For each location, a series of five hammer strikes were averaged to minimize noise. Figure 3 shows the layout of these accelerometer and driving point locations for later reference.

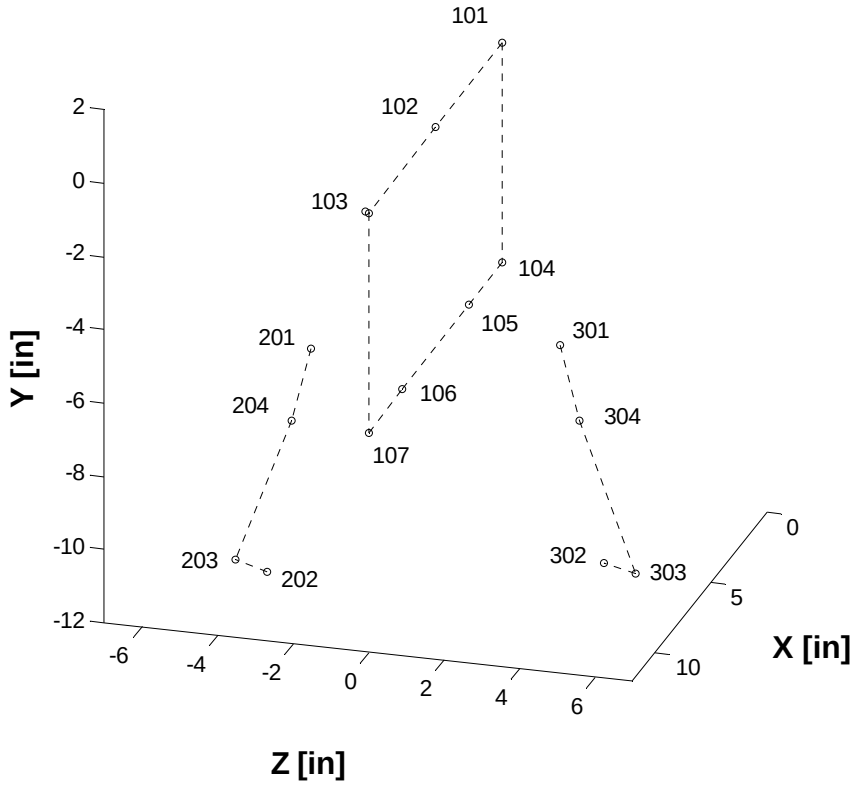

Figure 3. Matlab Generated Visualization of Catalytic Converter System

The measurements acquired in the linear modal tests were used to construct a composite frequency response function (FRF) for each driving point. These composite FRFs are shown in Fig. 4 providing a good indication of which modes are important in the system for each of the driving points. Here we can see that modes 1, 2, 3, 4 and 6 are dominated by Z-direction motion while mode 5 is more easily excited from the X-direction. After further investigation, the authors found modes 3 and 4 to be localized modes where only the heat shields moved significantly, and so those modes will be disregarded for this exercise as they do not contribute much to the dynamics of the assembly. Linear models for these modes could be readily added to the model if desired.

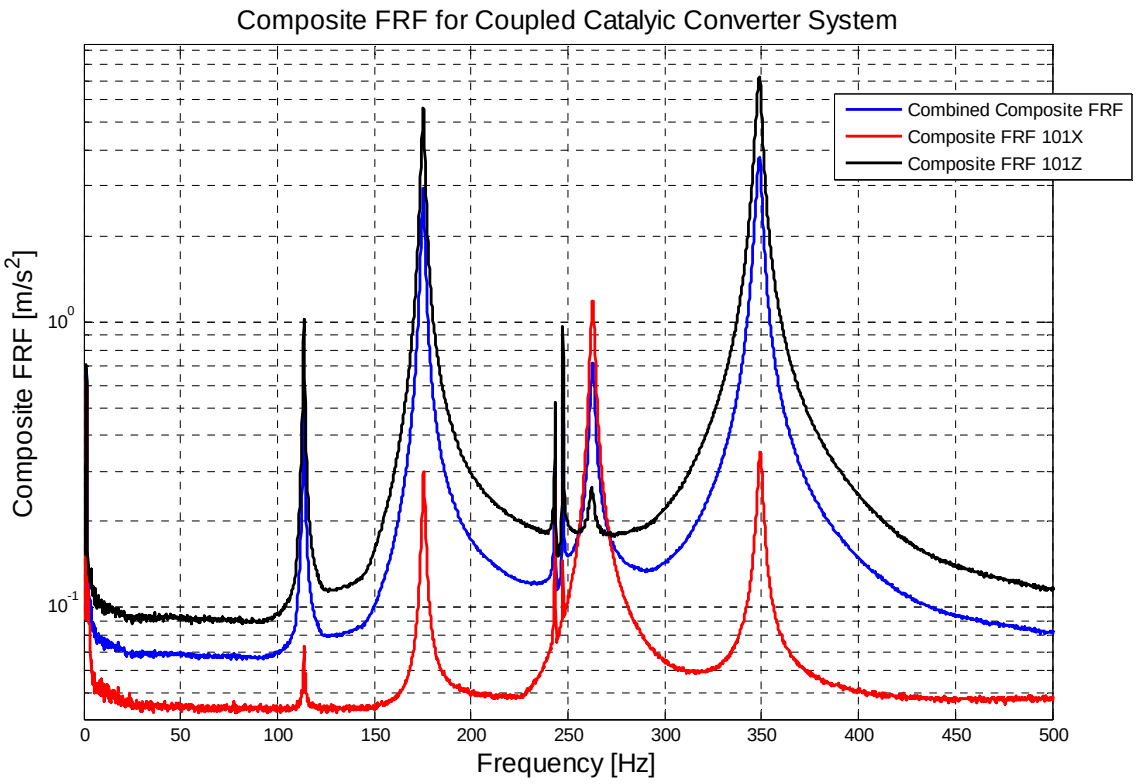

Figure 4. Composite FRF from Various Drive Points for Coupled Catalytic Converter System

Table 1 contains a list of the natural frequencies and damping ratios extracted for each of the modes using the Algorithm of Mode Isolation (AMI), a linear modal parameter identification algorithm that is detailed in [17]. The modes in this frequency range were found to include three bending modes, one torsional mode, and the two modes mentioned previously that are localized to the heat shields. Mode shapes for the global modes can be found in Appendix A.

Table 1: Linear (low amplitude) modal parameters

Modal Index	Natural Frequency [Hz]	Damping Ratio	Deflection Type
1	113.70	0.0030	Bending in Y-direction
2	175.42	0.0043	Bending in X-direction
3	243.41	0.0005	Localized Heat Shield Mode
4	247.38	0.0004	Localized Heat Shield Mode
5	262.71	0.0044	1st Torsion
6	348.68	0.0045	2nd Bending in Y-direction

4. Initial Screening – ZEFFT

The assembly was first probed using the ZEFFT, as discussed previously, to deduce whether any modes might behave nonlinearly. The structure was excited in the Z-direction at point 204 (see Fig. 3) with an impulsive

force with a peak of 506 N, and the response of Point 303-z was processed with the ZEFFT algorithm. Figure 5 shows the ZEFFT spectra of the assembly at point 303 in the z-direction (see Fig. 3); Fig. 5a shows the spectrum over the whole frequency range of interest; as is usually the case for structures with weak joint nonlinearities such as this, one must zoom in near each mode to discern any nonlinearity. Fig. 5b shows the ZEFFT near the first mode. The legends give the time t_n (see Eq. (1)), in milliseconds, at which the zeroed region ended for each curve. The resulting family of spectra show how nonlinear distortions increase as more of the early time (and hence higher amplitude and more nonlinear) parts of the time response are removed from the time history [8].

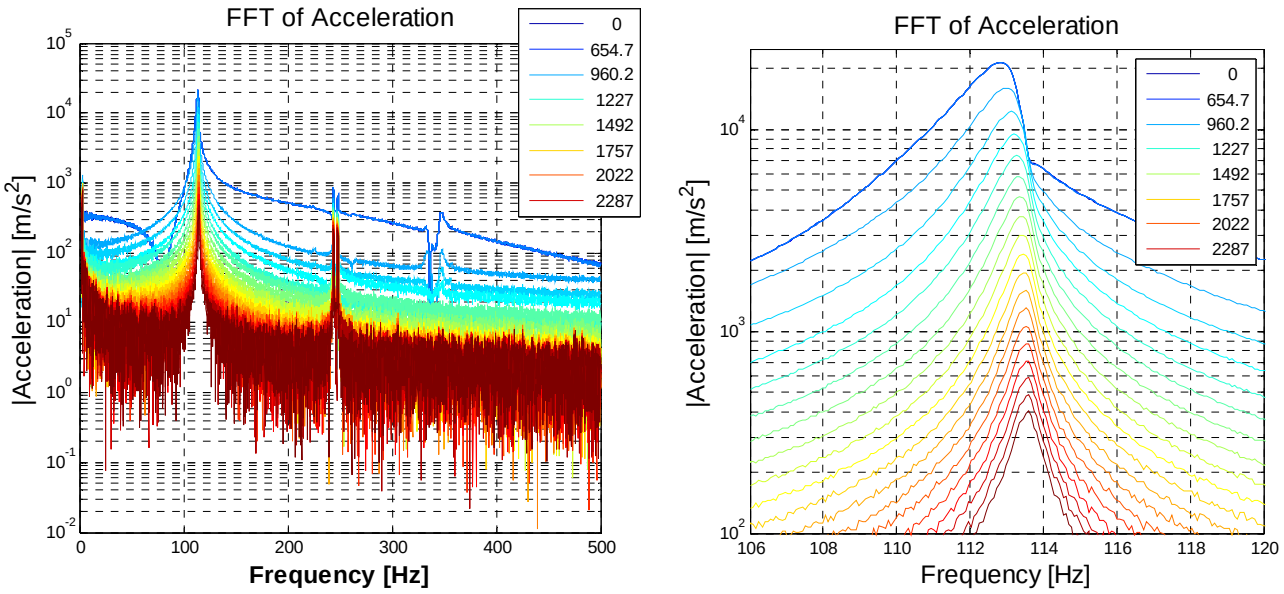

Figure 5. (a) Full ZEFFT spectra (b) Magnified View of ZEFFT spectra near 1st Resonance

The peak in the FFT occurs at a slightly lower frequency in the unzeroed response (denoted "0" in the legend) compared to that when the nonlinear portion of the response has been zeroed out (e.g. "1757 ms" in the legend), revealing that enough nonlinearity is present to cause about a 1.0 Hz (0.8%) shift in frequency. While this frequency shift shows that the stiffness nonlinearity is quite small, this mode exhibited much more significant nonlinearity in damping, as will be elaborated subsequently. It is also worth noting that the shape of the distorted spectrum in the early times in Fig. 5 is similar to what has been seen in other tests and simulations of structures with bolted joints [8, 18].

A similar analysis was performed on the second mode revealing a shift in the natural frequency of 0.4 Hz (0.2%) over the same range of input force. The ZEFFT near the second resonance at point 303 in the z-direction (see Fig. 3), obtained by exciting in the X-direction at point 204 with a peak force of 545 N, is shown in Fig. 6.

The magnified view in Fig. 6b also includes a second set of dashed lines that will be explained subsequently. Notice that the ZEFFT (solid lines in Fig. 6) does not show any strong evidence of nonlinearity. To check whether the response was indeed linear, the response at a lower amplitude was fit to a linear mode using the AMI algorithm and that fit was then extrapolated to earlier times to show how the spectrum should have appeared if the mode behaved linearly over this time span. This linear extrapolation is shown on in Fig. 6b with dashed lines, each corresponding to the same value of t_n as the solid lines from the ZEFFT algorithm. As discussed in [8], extrapolations such as these can often help when it is difficult to detect or make sense of a certain nonlinearity. These results show that the first two modes of the system do exhibit nonlinearity, but the first mode is more strongly excited and shows stronger nonlinearity.

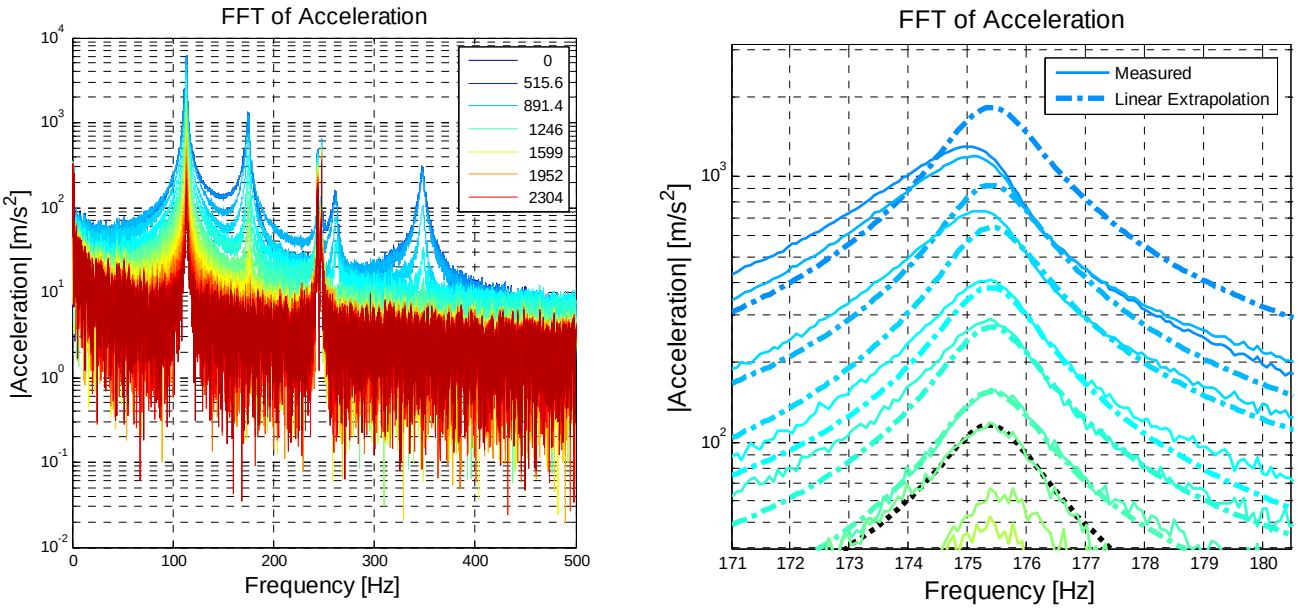

Figure 6. (a) Full ZEFFT spectra (b) Magnified View of ZEFFT spectra near 2nd Resonance

The response near the 5th and 6th modes was also examined as shown in Fig. 7, and while they seem to show traces of nonlinearity, it seemed negligible in these measurements. The forcing amplitude rolls off with increasing frequency, so either these modes are less susceptible to the nonlinearity induced by the joint or else the forcing is simply not adequate to excite nonlinearity in these modes. Based on the results of the ZEFFT analysis, the 1st and 2nd modes will be treated as nonlinear and the 5th and 6th will be treated as linear.

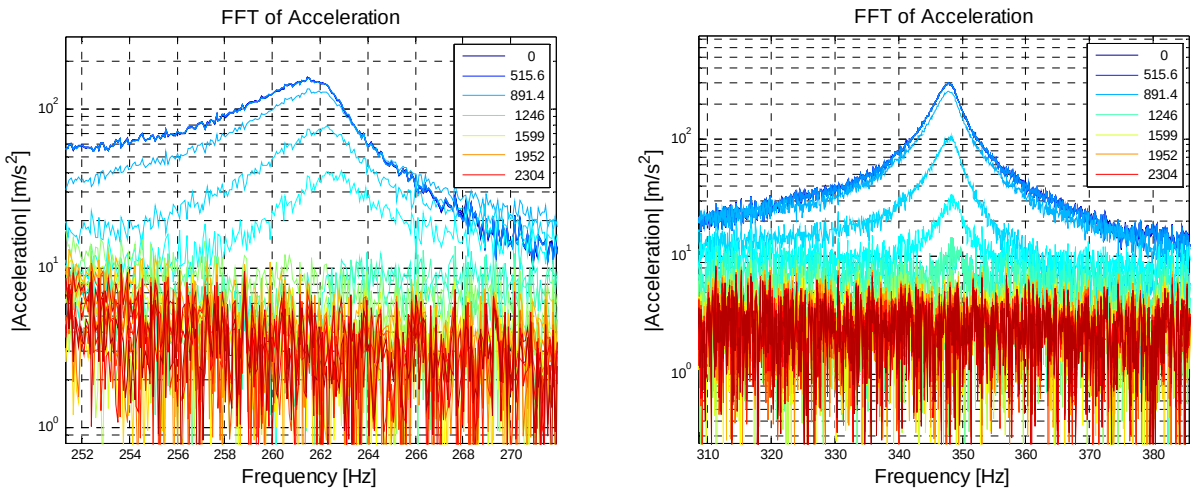

Figure 7. (a) ZEFFT spectra near 5th Resonance (b) ZEFFT spectra near 6th Resonance

5. Nonlinear Parameter Identification

After this initial screening with the ZEFFTs, the first two modes were characterized in more detail using the Hilbert transform approach discussed previously. Excitations were applied at several different points and at various amplitudes and then for each excitation the response at all of the accelerometers was used in Eq. (2) to obtain a least squares estimate the modal amplitude $q_1(t)$. Figure 8 shows the FFT of an experimental signal both from the modal filter and the band-pass filter. This band-pass filtered signal is the one used in the Hilbert transform.

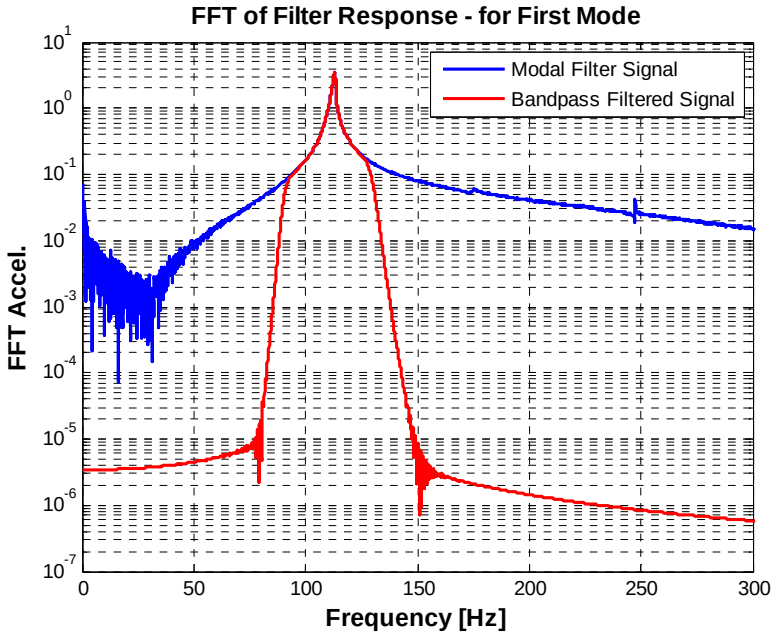

Figure 8. FFT of Filtered Signals

Using the Hilbert transform this signal was fit over a chosen time window based on the Hilbert amplitude and phase envelopes. As can be seen in Fig. 9 the signal often loses some early time data due to Hilbert transform end effects but the fit amplitude and phase construct a quality representation of the filtered modal acceleration from Eq. (3).

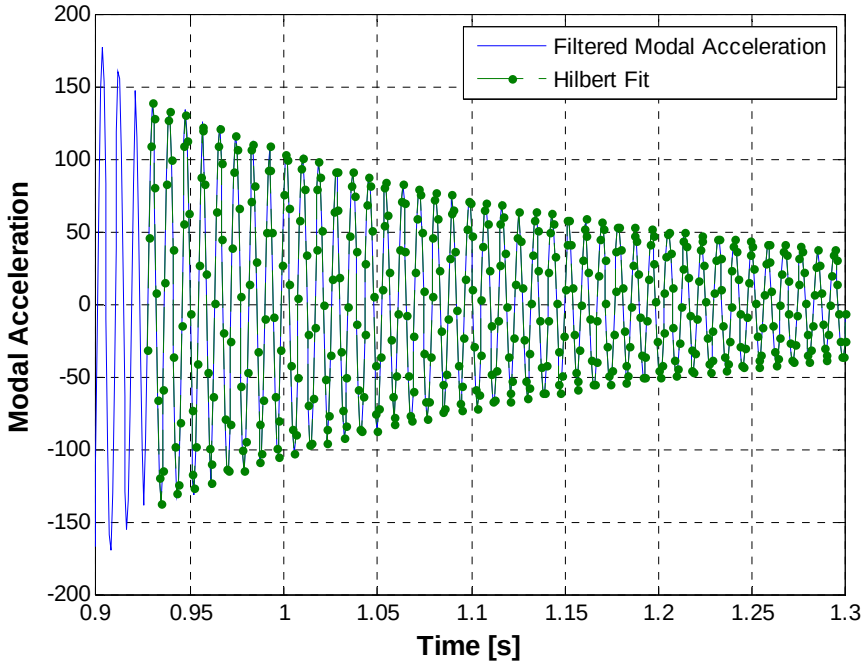

Figure 9. Filtered Modal Acceleration and Hilbert Fit of Signal

These were then processed as outlined in Sec. 2 and the resulting measured damping $\zeta_{meas}(t)$ was plotted against the velocity amplitude, $\left|\dot{Q}(t)\right|$, and the result is shown in Fig. 10. As mentioned previously, polynomials are fit to the analytic signal that the Hilbert transform produces, and while this dramatically reduces noise in the estimated damping, the smoothness of the polynomial fit can also make a spurious measurement appear to be physically meaningful. However, the spurious waviness at the lowest amplitudes (far left) is an artifact of the Hilbert transform and should be ignored. At higher amplitudes all of the curves agree remarkably well. All of the lines of the same colors were taken from the same excitation point but at different force levels. At the point where the curves show the most scatter, which is near an amplitude of 0.020 m/s, the damping ratio ranges from 0.0035 to 0.0037. This represents a variation of about 7% of the average value. The different line styles correspond to different input locations and/or directions. The various excitations at different forcing levels and locations all provide a similar modal damping vs. amplitude curve, especially at high amplitudes where the damping is not

constant but shows a power-law dependence on amplitude. Each excitation point excites a different combination of the modes, and hence the force across the joint would be different. Nevertheless, these results show that these complicating factors can be ignored and that this mode can be treated as single degree-of-freedom nonlinear system that is uncoupled from the other modes. Furthermore, the damping at high amplitudes is more than twice that at low amplitudes, so if this nonlinearity is not accounted for one might over predict the response of the structure by more than a factor of two. Additional impulses with even higher forces were applied using a heavy (non-instrumented) rubber mallet and the modal response curves extracted also agreed well with those shown. However, even with those large input forces it was difficult to obtain an estimate of the modal response at much higher amplitudes than those shown, presumably because of edge effects in the Hilbert transform and because the increased damping causes the response to decay more quickly.

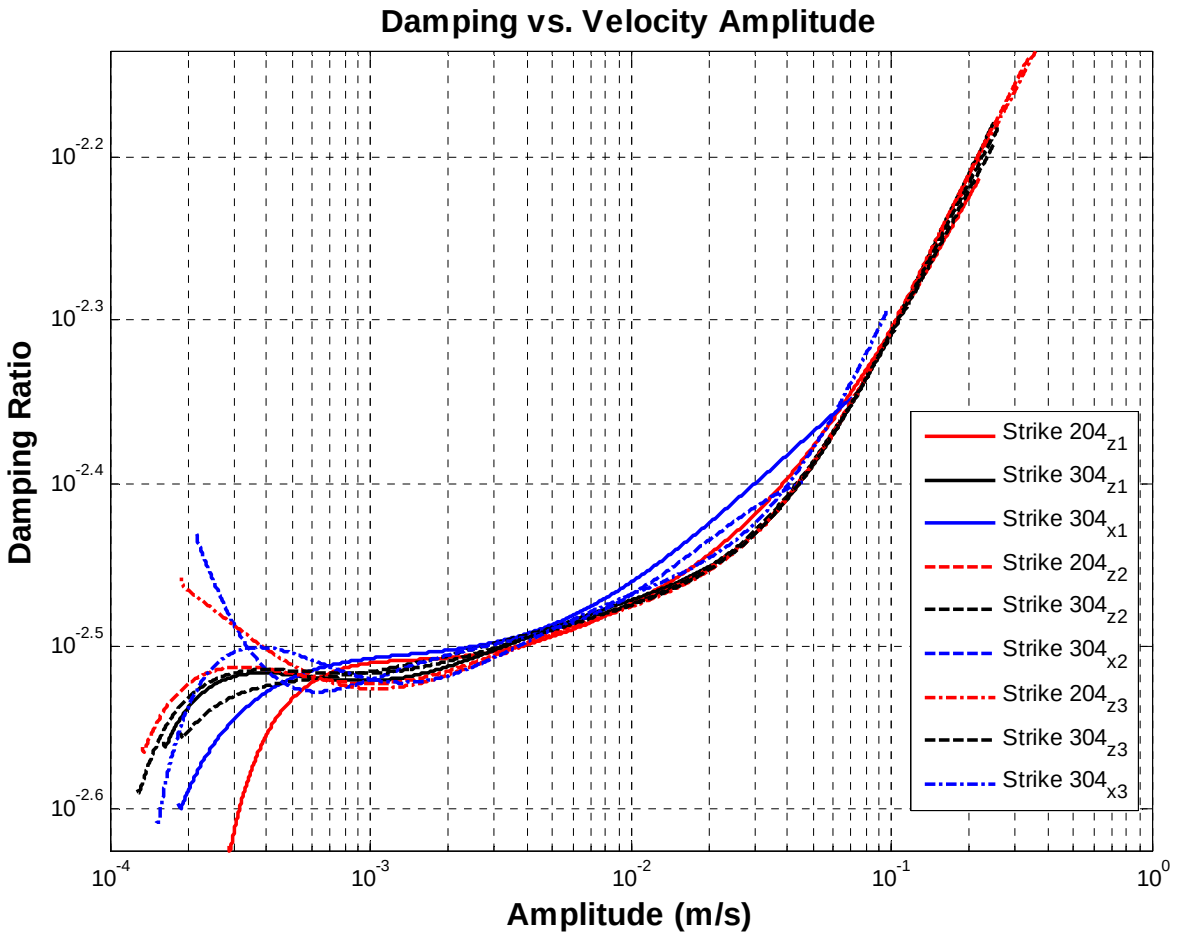

Figure 10. Damping ratio versus acceleration amplitude for 1st mode (Multiple Hammer Strikes)

This analysis was repeated for the second mode as well. Figure 11 shows the measured damping versus amplitude for several different hammer strikes. The Hilbert transform only produced useful data over a relatively small amplitude range for this mode, yet it still shows the power-law behavior that is characteristic of an Iwan model, with the damping increasing with amplitude according to a power-law relationship.

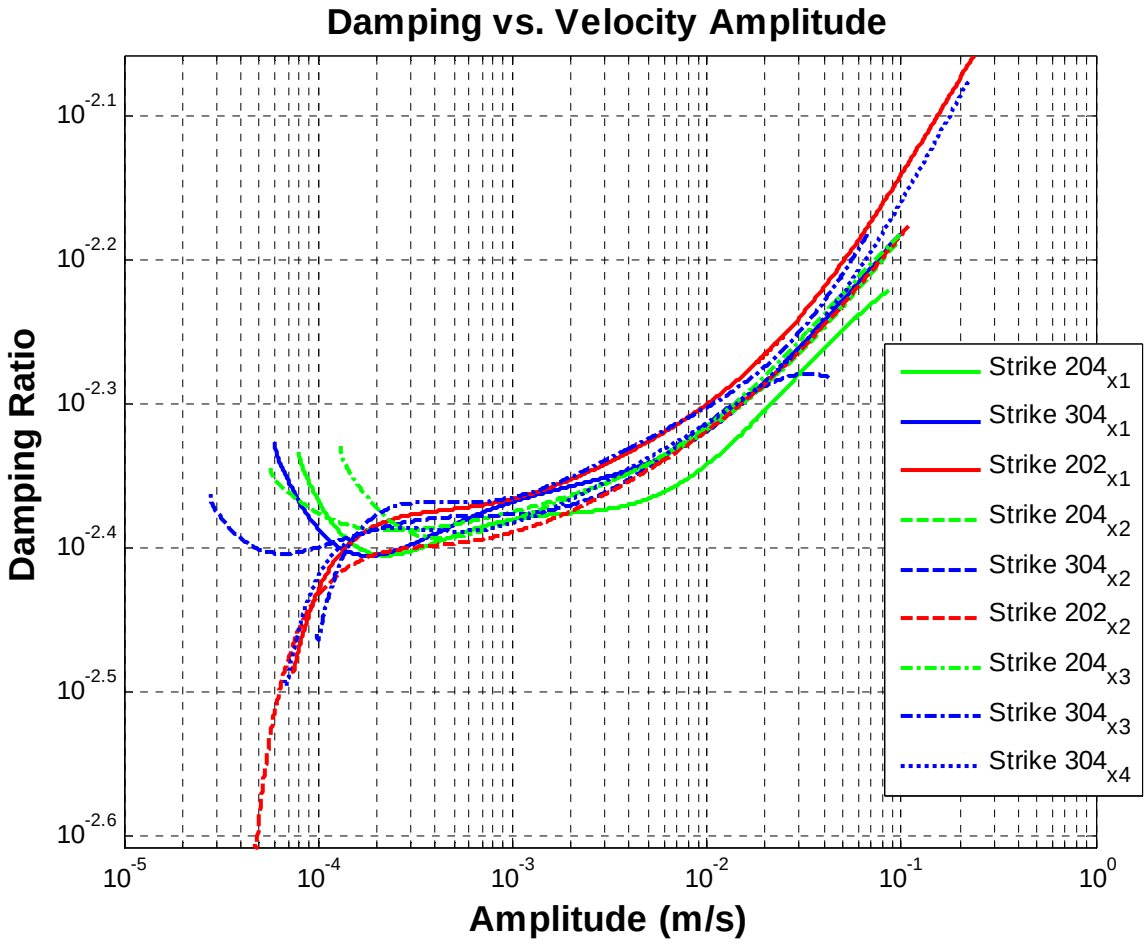

Figure 11. Damping ratio versus acceleration amplitude for 2nd mode (Multiple Hammer Strikes)

A summary of the observed frequency and damping nonlinearities is shown in Table 2. In contrast, the fifth and sixth modes were not excited enough to exhibit nonlinearity and will be modeled as linear.

Table 2: Summary of results for catalytic converter system NA = not applicable (linear mode)

Modal Index	Natural Frequency [Hz]	% Shift in Peak Frequency	Linear Damping Ratio	Maximum Damping Ratio	% Shift in Damping
1	113.70	0.8%	0.0030	0.0072	125.00%
2	175.42	0.2%	0.0043	0.0066	46.67%
5	262.71	NA	0.0044	NA	NA
6	348.68	NA	0.0045	NA	NA

The parameters of a modal Iwan model will now be estimated from the measurements for modes 1 and 2. There was no obvious evidence of macro-slip in the experimental test; therefore, the slip force can be assumed to be greater than any of the excitations applied experimentally.

$$F_S \geq \boldsymbol{\varphi}_{dp} F \tag{19}$$

The joint stiffness is related to the minimum and maximum stiffness that the mode has when the joint goes, respectively, from slipping completely to being perfectly locked. This parameter can be estimated based on the peak frequency shift observed using the ZEFFT algorithm. However, because macro-slip was not observed, one cannot know whether the frequency would shift further if even larger forces were applied.

The χ value can be calculated directly using the slope of the damping versus amplitude curve from Figs. 10 and 11. The χ value was difficult to estimate from Figs. 10 and 11 because the nonlinear Iwan damping was only dominant over part of the measurement. To address this, the linear damping ratio was subtracted from the instantaneous damping in Figs. 10 and 11 to isolate the nonlinear portion of the damping. This was then relatively easy to fit to a power law relationship as shown in Figure 12. For the first mode, the χ value was found to be $\chi = -0.280$.

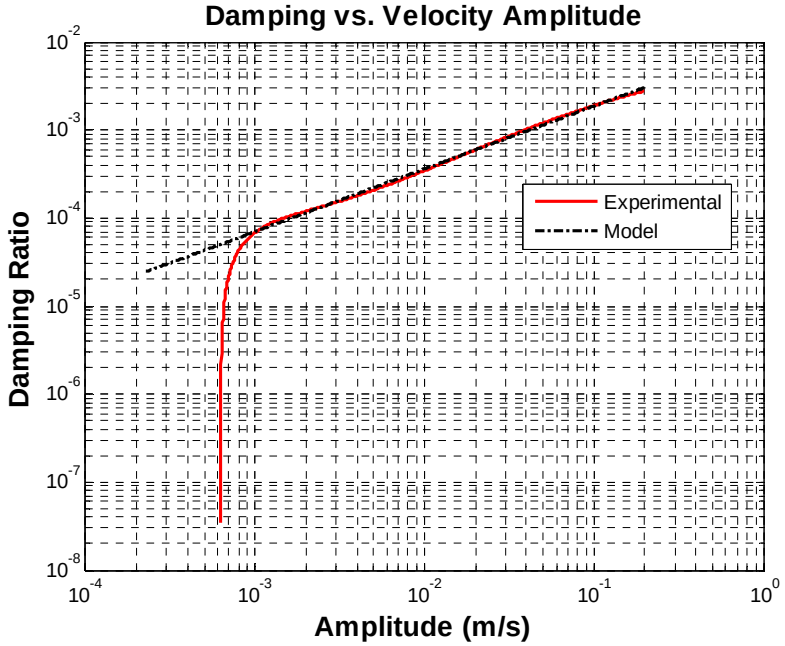

Figure 12. Damping Ratio versus acceleration amplitude for 1st mode after subtracting linear viscous damping of ζ_v=0.003.

In principle the parameter β can be found from the y-intercept of the dissipation versus amplitude curve, but in this case this would not be reliable since $\mathrm{F_s}$ and $\mathrm{K_T}$ were not known precisely. Instead β was assumed to be unity and then varied to see whether the results were sensitive to that assumption. These Iwan parameters can then be used to simulate the response of the mode in question to the measured impulse and then to compare the observed damping versus amplitude curves. Alternatively, one can use the approximate expressions derived in [2].

These concepts were used to estimate starting values for the parameters and then they were varied until the damping versus amplitude curve of the modal Iwan model, found by integrating the equation of motion with the Newmark algorithm [19], matched what was measured experimentally. The unknown parameters F_s and K_T were varied until the damping and frequency curves agreed. Figure 13 shows the damping versus amplitude and Fig. 14 shows the frequency versus velocity amplitude of the modal-Iwan model for the first mode. In this comparison, only a single hammer impact was used, and the measured impact force was applied to the modal-Iwan model to obtain a time domain simulation from which the damping versus amplitude and frequency versus time were extracted and which are labeled “Model” in Figs. 13 and 14. The simulation to generate these plots was completed using a forcing time history from a strike at location 204_{z1} (see Fig. 10).

Recall that K_T is calculated as a function of the natural frequency and the frequency shift using Eq. (13). It is interesting to note that the Hilbert transform of the simulated response clearly levels off at about 10^{-4} m/s but even for this noise free simulated data the damping estimated by the Hilbert Transform eventually shows spurious curvature below 10^{-6} m/s. This was found to be caused by edge effects in the FFT. The experimentally measured damping shows a strong spurious decrease below 10^{-3} m/s.

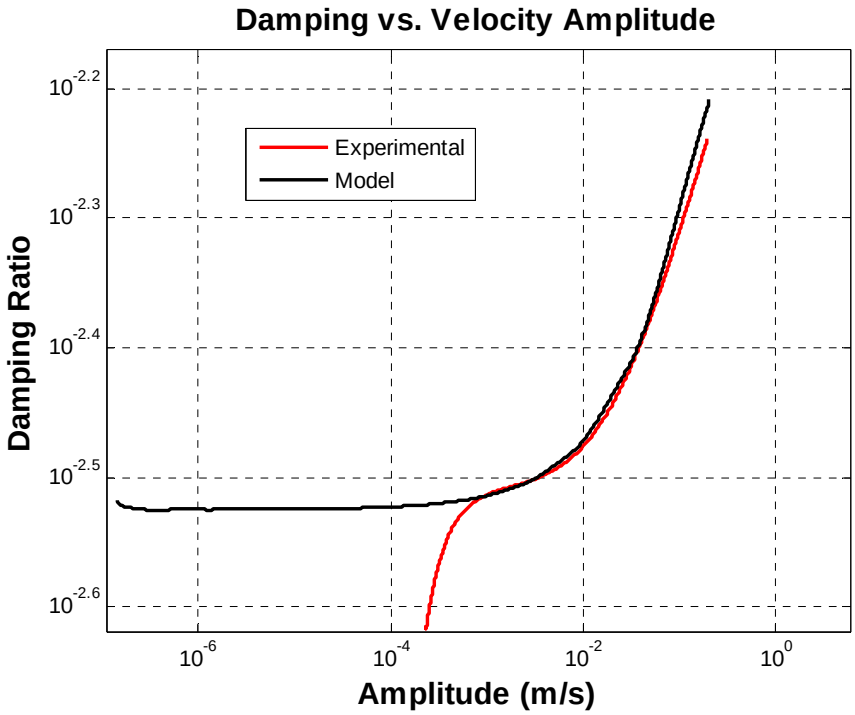

Figure 13. Damping Ratio versus Velocity Amplitude - 1st Mode

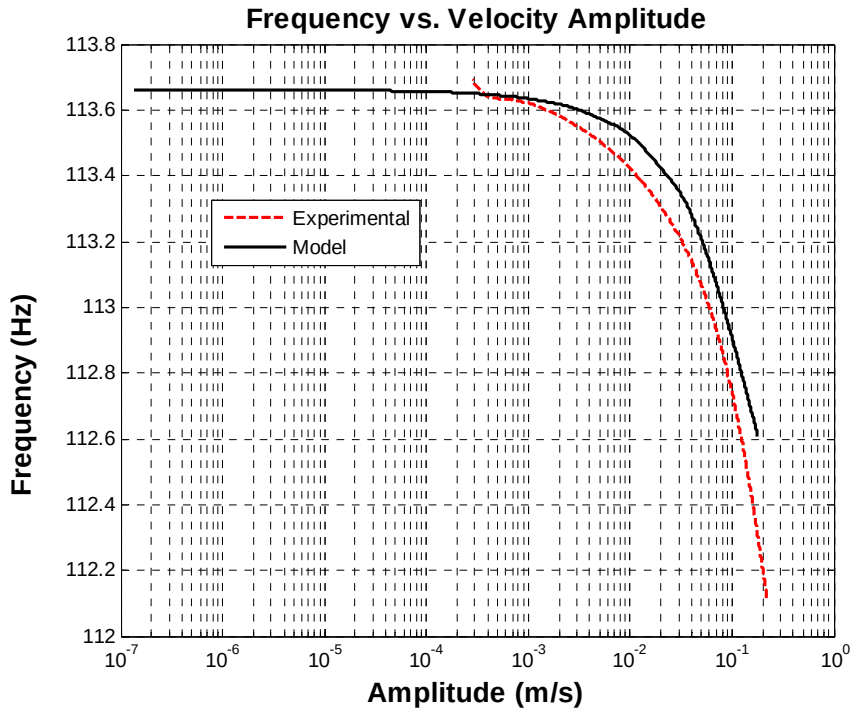

Figure 14. Frequency versus Velocity Amplitude - 1st Mode

A similar procedure was used for Mode 2 resulting in Figs. 15 and 16 . For this simulation the excitation at point 304_{x1} (see Fig. 11) was used to generate a response.

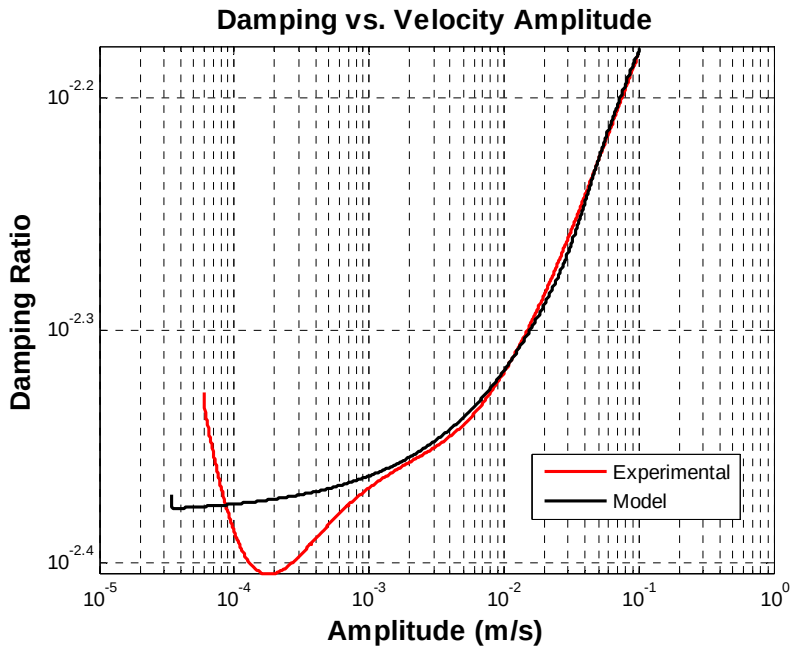

Figure 15. Damping Ratio versus Velocity Amplitude - 2nd Mode

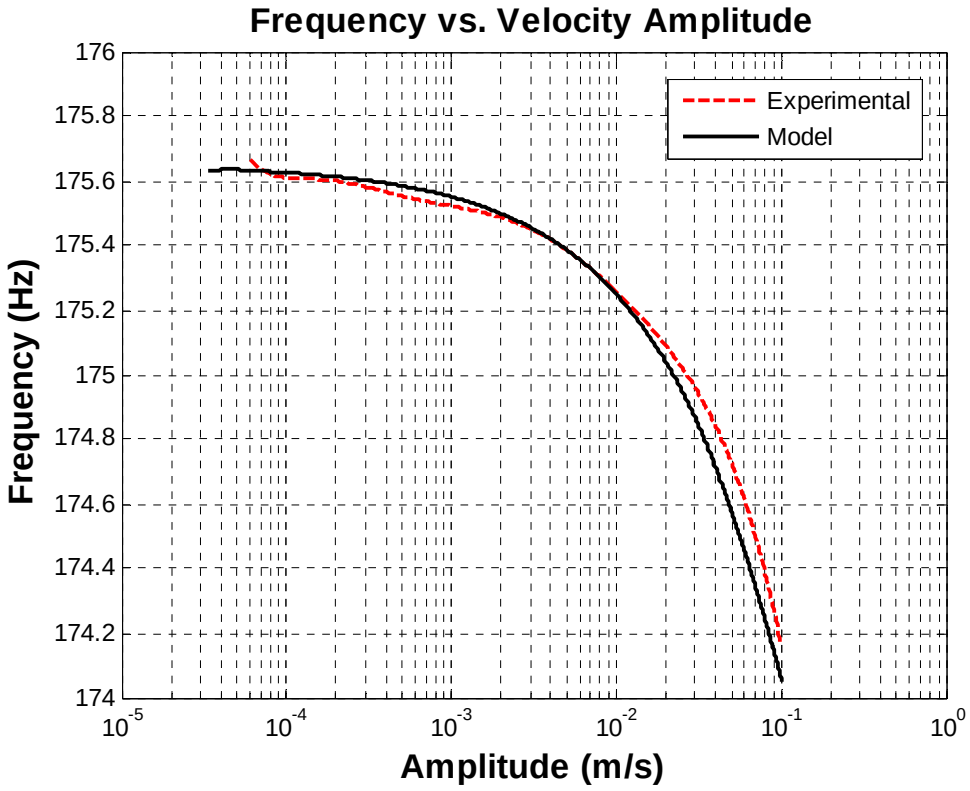

Figure 16. Frequency versus Velocity Amplitude - 2nd Mode

Table 3 shows the parameters that were used in simulations for modes 1 and 2..

Table 3: Iwan model parameters for catalytic converter system

Parameter	Simulation Case 1st Mode	Simulation Case 2nd Mode
F_s (N)	1200	1000
Δf_n (Hz)	40	41
K_T (N/m)	295930	501058
β	0.7	0.7
χ	-0.280	-0.400
Linear damping, Linear ζ_v	0.00305	0.0043

The Δf_n values here are much larger than those observed using the ZEFFT algorithm in Sec. 4. The amount of energy dissipated in the joint depends on how much load it carries. Hence, for the joint to cause the damping to change by a factor of two as was observed, it must carry significant load and the system experiences a large change in stiffness if the joints slips completely. Even then, this value is reasonable, since the frequency of the first mode would change quite dramatically if the bolts were not present. Indeed, in [5] the joint stiffness in a beam structure was estimated by loosening the bolts until they barely held the parts together and measuring the structure's natural frequencies.

The simulated response of these mode to the measured excitation is shown in Figs. 17 and 18 and excellent agreement was found with the measured modal response extracted from. The damping decays the signal at a similar rate and the frequency remains lined up throughout the decay even as it changes.

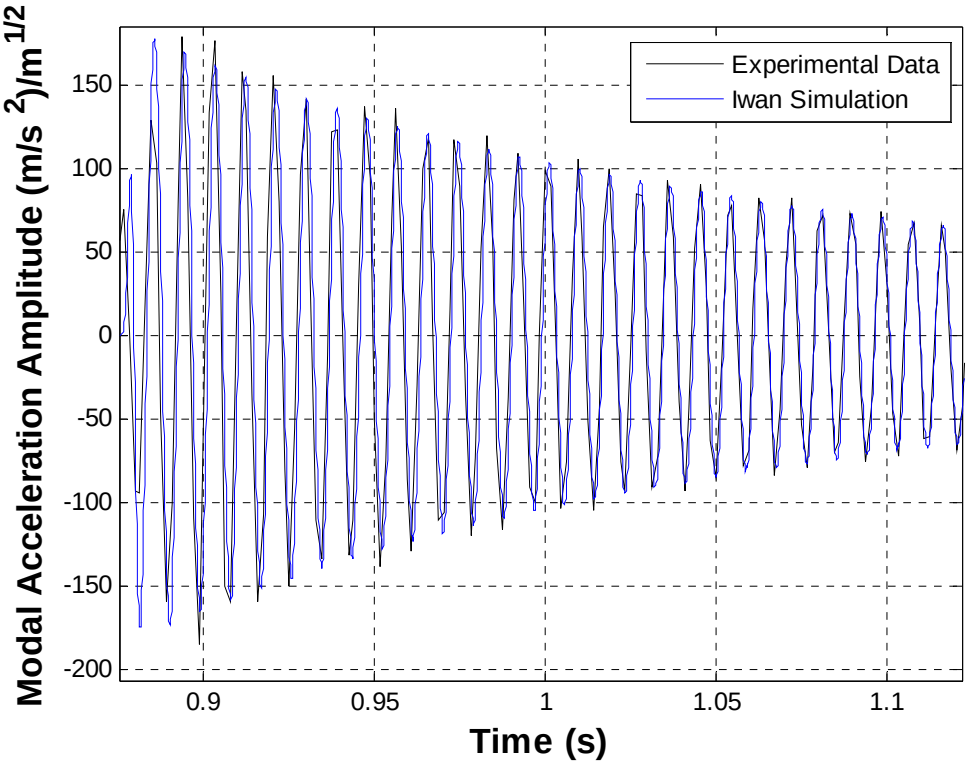

Figure 17. 1st Mode Acceleration Response (Experimental and Iwan Simulation)

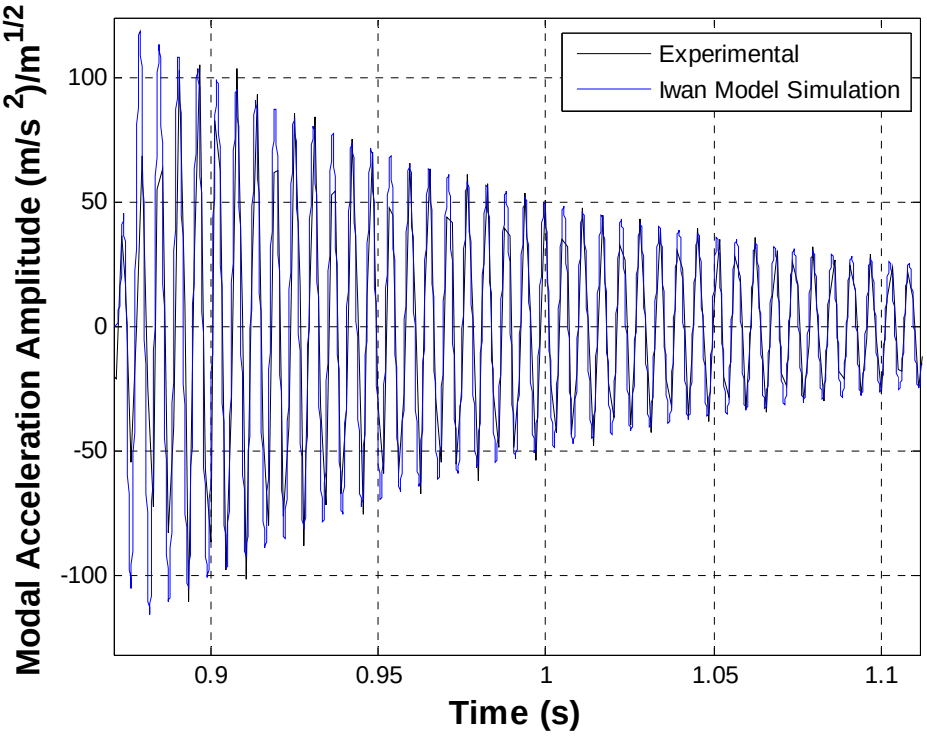

Figure 18. 2nd Resonance Modal Acceleration Response (Experimental and Iwan Simulation)

The two responses that were shown in Fig. 17 and 18 were from two different forces that excite each mode into the nonlinear regime, one could easily apply this procedure to a single force time history and add up all of the modal contributions to see the full response as was done in [5]. This comparison does not add any additional insight because the two modes combine in a complicated way so it was not shown.

6. Conclusions

This work explored the applicability of a Modal Iwan model to the first few modes of an assembly of actual production exhaust components. The results showed that the ZEFFT was useful in screening modes to determine which modes were most affected by joint nonlinearity. Then, a Hilbert transform analysis was used to quantify the change in damping with response amplitude and then to estimate the parameters of a nonlinear model for each mode. Using these tools, the procedure was relatively fast and could be readily extended to structures with many more modes. All of the modes of the assembly studied were either linear or well described by a modal Iwan model with a viscous damper in parallel to capture low-level material damping. It is encouraging that the Modal Iwan framework seems to be capable of describing all of these lower modes of this structure, and it was relatively easy to characterize the structure mode-by-mode in this manner. It would have been much more challenging to model each joint as a discrete nonlinearity and then to update a model for the entire structure to try to obtain the behavior that was observed in the measurements, and the resulting model would be more expensive to integrate.

Appendix A: Mode Shapes for Global Modes

This appendix contains visualizations of the global mode shapes using stick models. Here, one can see thee first mode as a bending mode of the system with the catalytic converters out of phase with one another. In the second mode the converters are in phase as the plate rotates. The fifth mode is a torsional mode as the plate and converts twist about the z-directional axis. The sixth mode is a second bending mode causing the plate to rotate about the other planar x-direction axis.

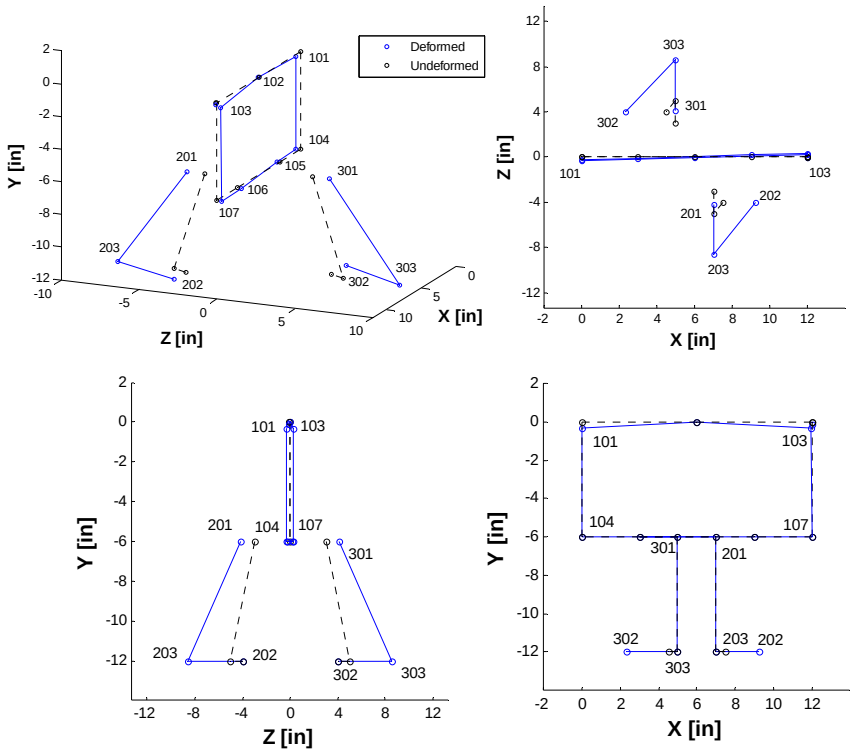

Figure 19. 1st Mode Visualization

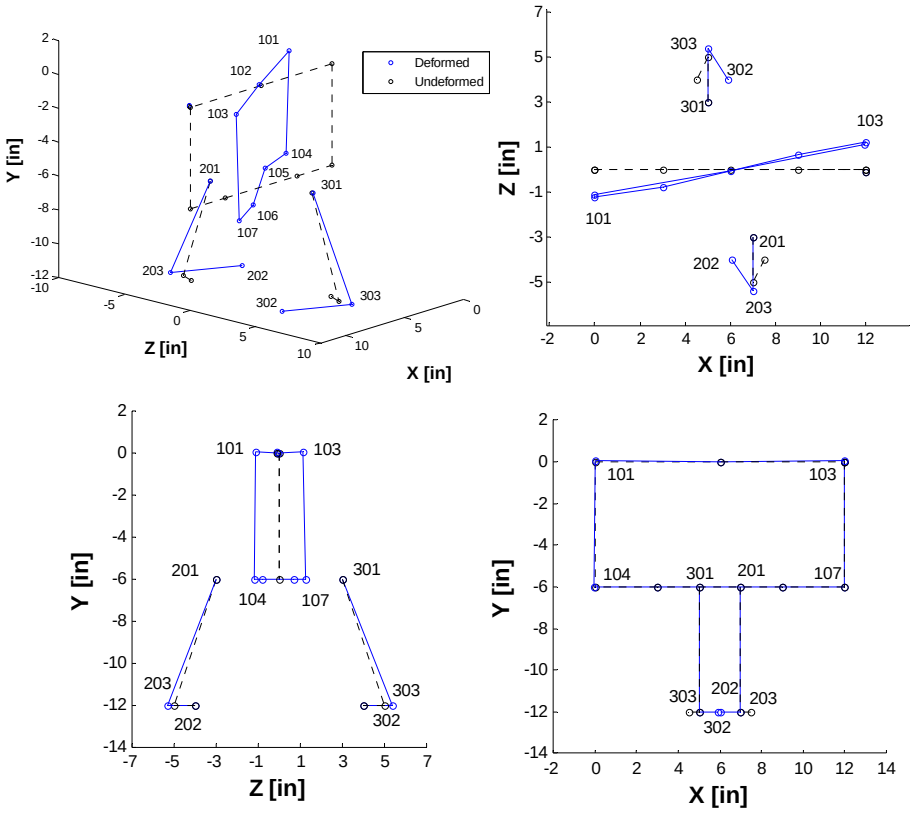

Figure 20. 2nd Mode Visualization

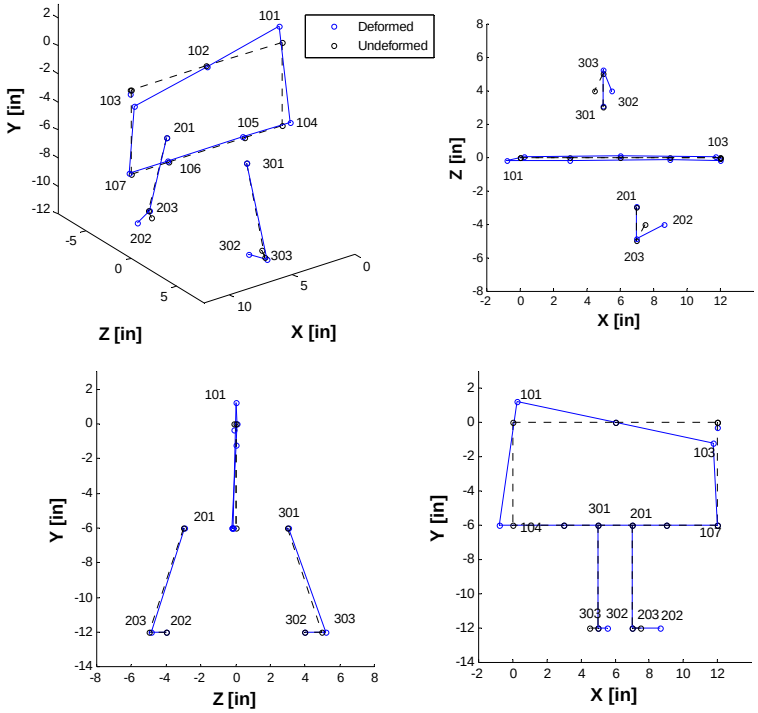

Figure 21. 5th Mode Visualization

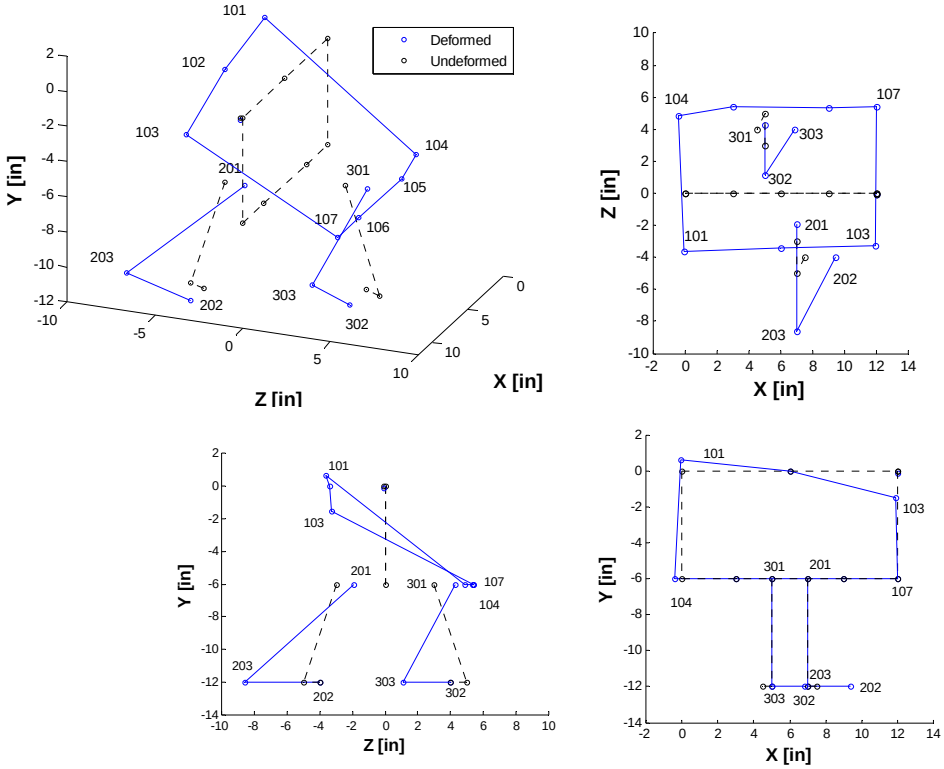

Figure 22. 6th Mode Visualization

Acknowledgements

This work was conducted / supported by Sandia National Laboratories. Sandia is a multi-program laboratory operated under Sandia Corporation, a Lockheed Martin Company, for the United States Department of Energy under Contract DE-AC04-94-AL85000.

References

[1] D. J. Segalman, "An Initial Overview of Iwan Modelling for Mechanical Joints," Sandia National Laboritories, Albuquerque, New Mexico SAND2001-0811, 2001.

[2] D. J. Segalman, "A Four-Parameter Iwan Model for Lap-Type Joints," *Journal of Applied Mechanics,* vol. 72, pp. 752-760, September 2005.

[3] D. J. Segalman, "A Modal Approach to Modeling Spatially Distributed Vibration Energy Dissipation," Sandia National Laboratories, Albuquerque, New Mexico and Livermore, California SAND2010-4763, 2010.

[4] M. Eriten*, et al.*, "Nonlinear system identification of frictional effects in a beam with a bolted joint connection," *Mechanical Systems and Signal Processing,* vol. 39, pp. 245-264, 2013.

[5] B. Deaner, Allen, M. S., Starr, M.J., Segalman, D.J., and Sumali, H., "Application of Viscous and Iwan Modal Damping Models to Experimental Measurements From Bolted Structures," *ASME Journal of Vibration and Acoustics,* vol. 137, 2015 2015.

[6] B. Deaner*, et al.*, "Investigation of Modal Iwan Models for Structures with Bolted Joints," presented at the 31st International Modal Analysis Conference (IMAC XXXI), Garden Grove, CA, 2013.

[7] M. W. Sracic*, et al.*, "Identifying the modal properties of nonlinear structures using measured free response time histories from a scanning laser Doppler vibrometer," presented at the 30th International Modal Analysis Conference Jacksonville, Florida, 2012.

[8] M. S. Allen and R. L. Mayes, "Estimating the Degree of Nonlinearity in Transient Responses with Zeroed Early-Time Fast Fourier Transforms," *Mechanical Systems and Signal Processing,* vol. 24, pp. 2049–2064, 2010.

[9] S. Braun and M. Feldman, "Decomposition of non-stationary signals into varying time scales: Some aspects of the EMD and HVD methods," 2011.

[10] G. Kerschen*, et al.*, "Toward a fundamental understanding of the Hilbert-Huang transform in nonlinear structural dynamics," *JVC/Journal of Vibration and Control,* vol. 14, pp. 77-105, 2008.

[11] M. Feldman, "Non-linear system vibration analysis using Hilbert transform--I. Free vibration analysis method 'Freevib'," *Mechanical Systems and Signal Processing,* vol. 8, pp. 119-127, 1994.

[12] T. P. Sapsis*, et al.*, "Effective stiffening and damping enhancement of structures with strongly nonlinear local attachments," *Journal of Vibration and Acoustics, Transactions of the ASME,* vol. 134, 2012.

[13] S. Bograd*, et al.*, "Modeling the dynamics of mechanical joints," *Mechanical Systems and Signal Processing,* vol. 25, pp. 2801-2826, 2011.

[14] D. Suc and K. Willner, "Multiharmonic balance analysis of a jointed friction oscillator," in *6th European Congress on Computational Methods in Applied Sciences and Engineering, ECCOMAS 2012, September 10, 2012 - September 14, 2012*, Vienna, Austria, 2012, pp. 1907-1914.

[15] D. J. Ewins, *Modal Testing: Theory, Practice and Application*. Baldock, England: Research Studies Press, 2000.

[16] D. R. Roettgen*, et al.*, "Feasibility of Describing Joint Nonlinearity in Exhaust Components with Modal Iwan Models," presented at the ASME International Design Engineering Technical Conference, Buffalo, NY, 2014.

[17] M. S. Allen and J. H. Ginsberg, "A Global, Single-Input-Multi-Output (SIMO) Implementation of The Algorithm of Mode Isolation and Applications to Analytical and Experimental Data," *Mechanical Systems and Signal Processing,* vol. 20, pp. 1090–1111, 2006.

[18] B. Deaner, "Modeling the Nonlinear Damping of Jointed Structures Using Modal Models," M.S., Engineering Physics, University of Wisconsin-Madison, Madison, WI, 2013.

[19] R. D. Cook*, et al.*, *Concepts and Applications of Finite Element Analysis*, 4th Edition ed. New York: Wiley, 2002.